Acquiring Record Barrier Height for Magnetization Reversal in Lanthanide Encapsulated Fullerene Molecules Using DFT and *Ab initio* Calculations

Mukesh Kumar Singh and Gopalan Rajaraman*

Department of Chemistry, Indian Institute of Technology Bombay, Mumbai-400076, India.
E-mail: rajaraman@chem.iitb.ac.in; Tel:+91-22-2576-7187

Here we have chosen a systematic DFT and *ab* initio study on several reported La@EMF complexes. Our calculations suggest, $\{Dy(III)\text{-}O\text{-}Sc(III)\}^{4+}$ as the best guest which yields superior SMM characteristics with all twelve fullerene cages tested, and C_{82} as the best host as this yield superior SMM properties with record U_{cal} of 1406 cm^{-1}. This is one of the largest U_{cal} estimated till date and all the model possesses very large barrier height suggest that these class of molecule has large potential to exhibit magnetization blockade and hence need to reach audience working in the area of molecular magnetism, lanthanide chemistry, endohedral fullerene, supra-molecular chemistry, host-guest interactions to assess and employ the strategy to generate new generation SMMs.

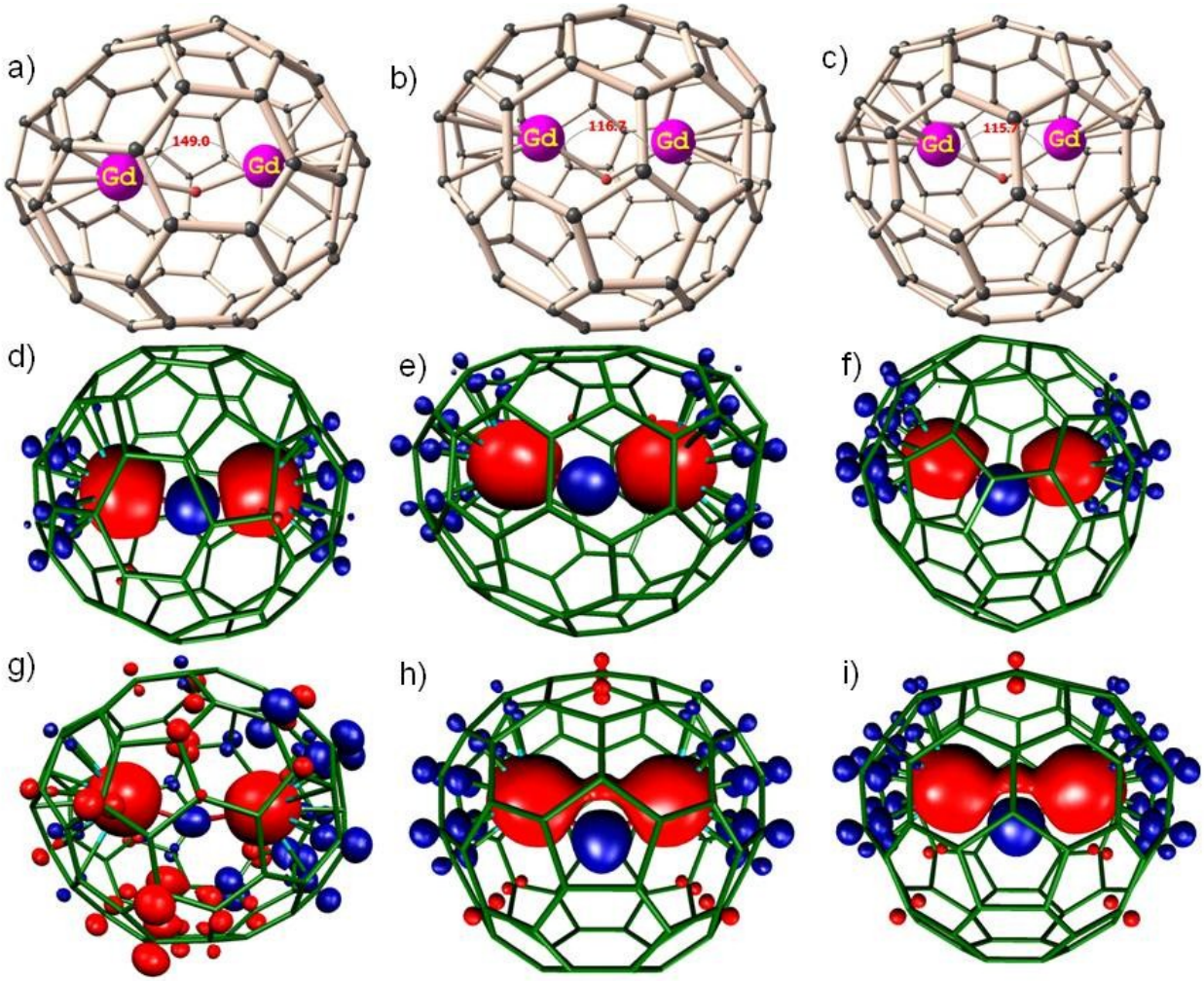

Figure S1. *DFT optimized structures for a) $Gd_2O@C_{76}$-2; b) $Gd_2O@C_{76}$-3 and c) $Gd_2O@C_{76}$-4 along with calculated spin density plots for d) Gd2O@C72; e) Gd2O@C76-1; f) Gd2O@C82; g) Gd2O@C76-2; h) Gd2O@C76-3 and i) Gd2O@C76-4. Colour scheme; Gd^{III}, pink; O, red and C, light grey. Red and blue regions indicate positive and negative spin populations, respectively. The isodensity surface shown corresponds to a value of 0.003 $e^-/bohr^3$ for $Gd_2O@C_{76}$(2) and 0.0005 $e^-/bohr^3$ for all other EMFs.*

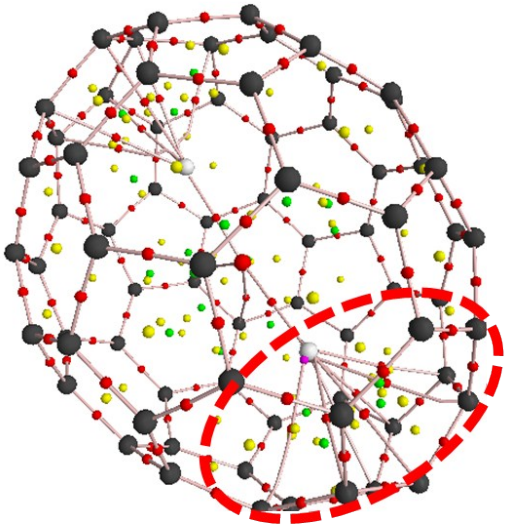

$Gd_2O@C_{72}$

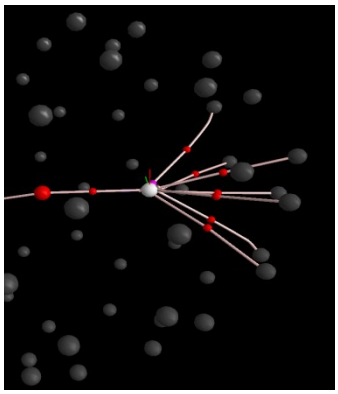

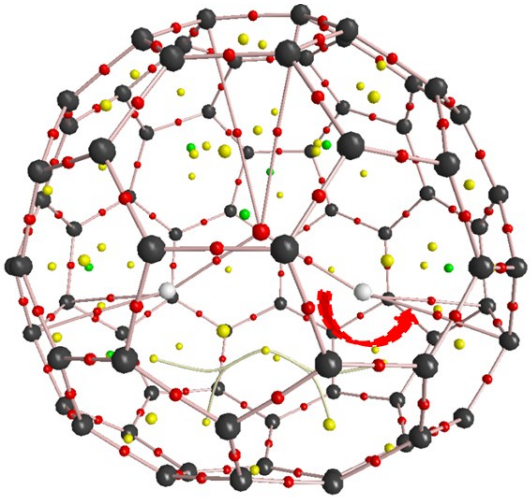

$Gd_2O@C_{76}$

O-Gd-C = 150-160°

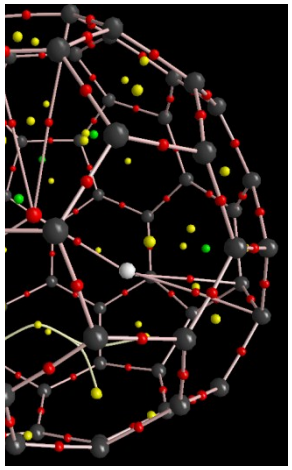

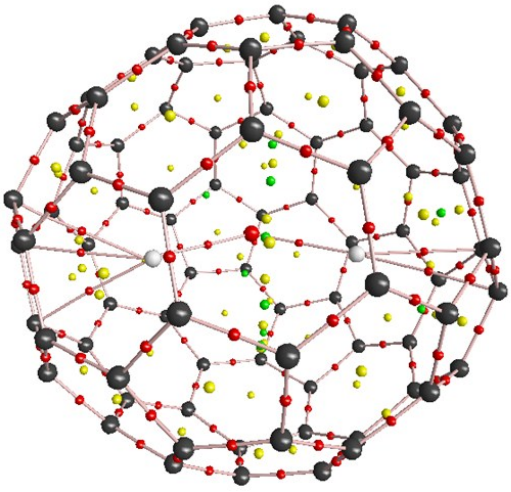

$Gd_2O@C_{82}$

O-Gd-C = 178°

O-Gd-C = 158°

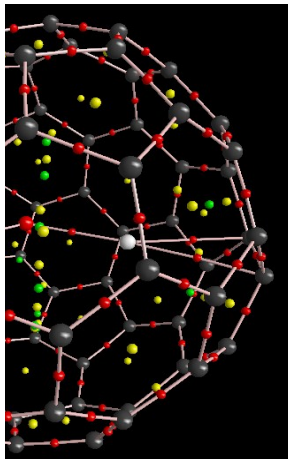

Figure S2. AIM analysis performed on $Gd_2O@C_{72}$, $Gd_2O@C_{76}$ and $Gd_2O@C_{82}$ (top to bottom respectively) to show the ligand field environment in all these complexes. Trend for deviation of interacting ligand field from ideal axial ligand field environment is found to be $DyOLu@C_{82}$ < $DyOLu@C_{76}(4)$ < $DyOLu@C_{72}$.

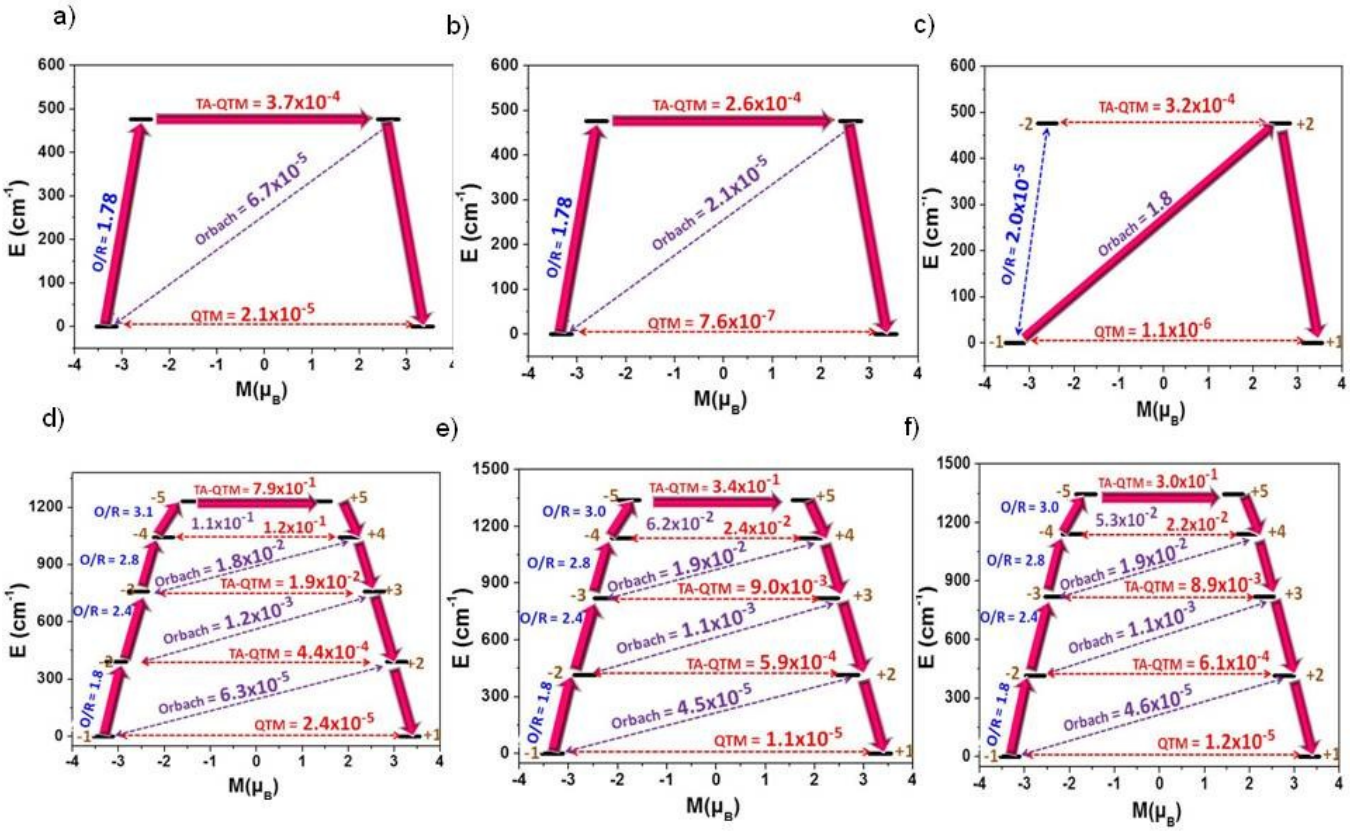

Figure S3. *Ab initio SINGLE_ANISO computed magnetization blockade barrier for a)* DyOLu@C_{76}*-2; b)* DyOLu@C_{76}*-3 c)* DyOLu@C_{76}*-4; d) DyOSc@C_{76}-2; e) DyOSc@C_{76}-3 and f) DyOSc@C_{76}-4*. The x- axis indicates the magnetic moment of each state along the main magnetic axis while y- axis denotes the energy of the respective states. The thick black lines imply the Kramer's doublet as a function of magnetic moment. The dotted indigo lines indicate the possible pathway of the Orbach/Raman contribution of magnetic relaxation. The solid pink arrows indicate the most probable relaxation pathway for the magnetization reorientation. The dotted orange lines correspond to the QTM/TA-QTM/Δtunneling relaxation contributions between the connecting pairs. The numbers provided at each arrow are the mean value for the corresponding matrix element of the magnetic moment.*

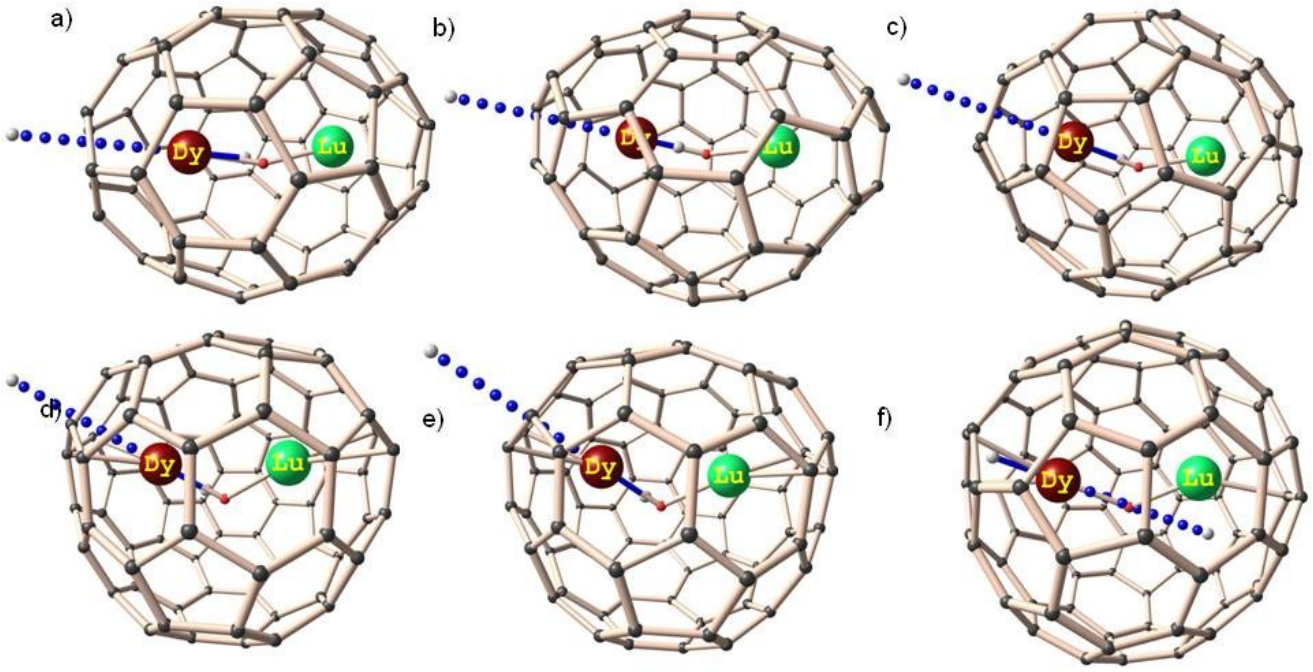

Figure S4. *Ab initio SINGLE_ANISO computed ground state KD orientation for a)* DyOLu@C_{76}*-2; b)* DyOLu@C_{76}*-3 c)* DyOLu@C_{76}*-4; d) DyOSc@C_{76}-2; e) DyOSc@C_{76}-3 and f) DyOSc@C_{76}-4.

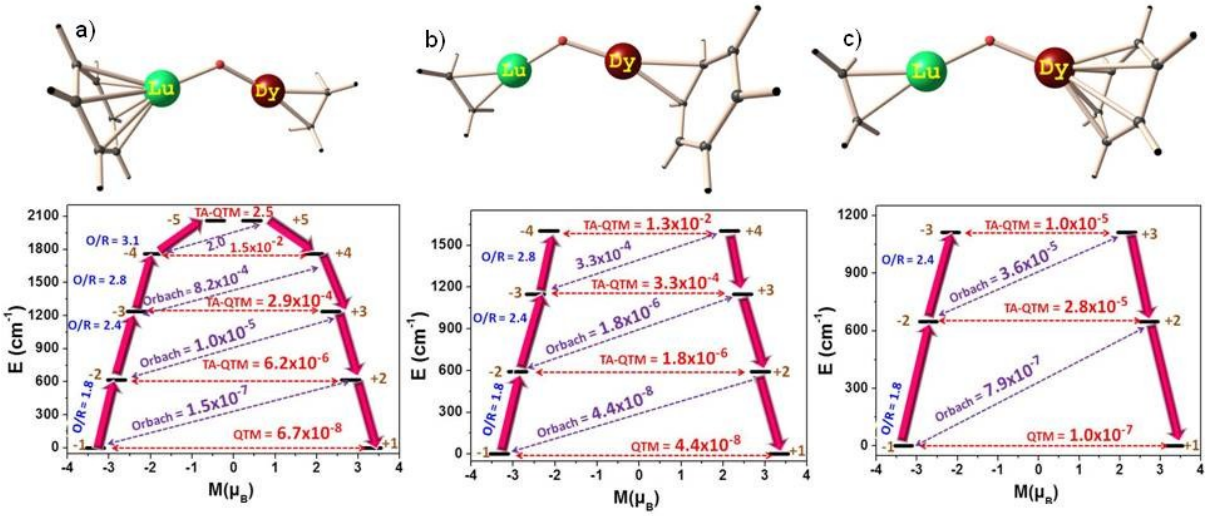

Figure S5. *Ab initio SINGLE_ANISO computed magnetization blockade barrier for a)* Model a*; b)* Model b *and c) Model c. The x- axis indicates the magnetic moment of each state along the main magnetic axis while y- axis denotes the energy of the respective states. The thick black lines imply the Kramer's doublet as a function of magnetic moment. The dotted indigo lines indicate the possible pathway of the Orbach/Raman contribution of magnetic relaxation. The solid pink arrows indicate the most probable relaxation pathway for the magnetization reorientation. The dotted orange lines correspond to the QTM/TA-QTM/Δtunneling relaxation contributions between the connecting pairs. The numbers provided at each arrow are the mean value for the corresponding matrix element of the magnetic moment.*

Table S1. Important structural parameters for optimized di-lanthanide EMFs. Relative energies for all the four isomers of $Gd_2O@C_{76}$ are also reported

Molecules	Gd1-O (Å)	Gd2-O (Å)	Gd1-O-Gd2 (Å)	Gd-Gd (Å)	J cm^{-1}	Relative Energies (kJ/mol)
Gd_2O-C_{72}	2.03	2.03	157.8	3.98	-0.21(-0.15)	
Gd_2O-C_{76}-1	2.06	2.06	150.2	3.98	0.15(0.11)	0.0
Gd_2O-C_{76}-2	2.06	2.03	149.0	3.94	-0.23(-0.16)	6.2
Gd_2O-C_{76}-3	2.05	2.05	116.7	3.49	0.41(0.29)	41.1
Gd_2O-C_{76}-4	2.05	2.05	117.8	3.51	0.45(0.32)	55.2
Gd_2O-C_{82}	2.07	2.05	129.7	3.72	-0.01(-0.01)	

Table S2. *Bond critical point (BCP) properties in $Gd_2O@C_{72}$, $Gd_2O@C_{76}$-4 and $Gd_2O@C_{82}$ molecules. AIM analysis was performed at the same computational level as used for single point calculations. [a]The electron density at the bond critical point (BCP). [b]The Laplacian of the electron density at the BCP. [c]The electronic kinetic energy density [d]The total energy density at the BCP.*

Gd_2O-C_{72}	O-Gd-C angle	Gd-C/O (Å)	$\rho(r)^a$ (ea_0^{-3})	$\nabla^2\rho(r)^b$(ea_0^{-5})	$G(r)^c$(ea_0^{-1})	$H(r)^d$(ea_0^{-4})
Gd1-C10	128	2.625	0.03948	0.13845	0.03629	-0.00168
Gd1-C6	146	2.577	0.04258	0.14354	0.03917	-0.00328
Gd1-C3	152	2.606	0.04190	0.14801	0.03961	-0.00261
Gd1-C2	176	2.595	0.04276	0.15409	0.04102	-0.00250
Gd1-C7	128	2.595	0.04098	0.13868	0.03743	-0.00276
Gd1-C11	125	2.611	0.04046	0.13772	0.03684	-0.00241
Gd1-O		2.026	0.12103	0.54595	0.16543	-0.02895

Gd_2O-C_{76}-4	O-Gd-C angle	Gd-C/O (Å)	$\rho(r)^a$ (ea_0^{-3})	$\nabla^2\rho(r)^b$(ea_0^{-5})	$G(r)^c$(ea_0^{-1})	$H(r)^d$(ea_0^{-4})
Gd1-C57	154	2.460	0.0545	0.17766	0.05190	-0.00749
Gd1-C58	154	2.460	0.0545	0.18595	0.05365	-0.00716
Gd1-O		2.057	0.1127	0.53947	0.15889	-0.02402

Gd_2O-C_{82}	O-Gd-C angle	Gd-C/O (Å)	$\rho(r)^a$ (ea_0^{-3})	$\nabla^2\rho(r)^b$(ea_0^{-5})	$G(r)^c$(ea_0^{-1})	$H(r)^d$(ea_0^{-4})
Gd1-C22	153	2.454	0.0553	0.182824	0.05382	-0.00812
Gd1-C13	173	2.489	0.0515	0.177506	0.05022	-0.00584
Gd1-O		2.063	0.1103	0.511019	0.14960	-0.02184

Table S3. *CASSCF+RASSI-SO computed relative energies of eight low lying KDs and g tensors of eight low lying KDs for* DyOLu@C_{72}*-2,* DyOLu@C_{72}*-3 and* DyOLu@C_{72}*-4 molecules, along with deviations from the principal magnetization axes of the first KD.*

M	DyOLu@C_{76}-2			DyOLu@C_{76}-3			DyOLu@C_{76}-4		
	E cm^{-1}	gx, gy, gz	(°)	E cm^{-1}	gx, gy, gz	(°)	E cm^{-1}	gx, gy, gz	(°)
1	0.0	0.00, 0.000, 19.961		0.0	0.000, 0.00, 19.982		0.0	0.000, 0.00, 19.981	
2	425.7	0.001, 0.001, 17.100	4.7	487.0	0.001, 0.001, 17.101	6.9	476.6	0.001, 0.001, 17.099	173.7
3	830.9	0.049, 0.056, 14.29	5.9	893.3	0.075, 0.084, 14.25	6.6	886.7	0.070, 0.078, 14.25	174.2
4	1153.3	0.213, 0.295, 11.519	1.8	1206.3	0.074, 0.180, 11.518	179.5	1204.3	0.029, 0.127, 11.517	0.6
5	1349.0	2.306, 2.521, 8.238	6.6	1401.5	1.604, 1.791, 9.620	24.9	1403.7	1.245, 1.497, 9.443	22.3
6	1429.0	10.575, 6.970, 2.728	2.0	1488.6	3.412, 4.214, 11.814	106.8	1489.0	3.316, 4.988, 11.962	74.2
7	1490.7	0.658, 2.489, 14.919	90.2	1568.9	7.271, 6.493, 1.383	167.9	1564.7	8.889, 5.342, 1.424	174.0
8	1534.4	0.017, 3.390, 16.198	88.1	1615.6	11.064, 9.770, 1.011	170.9	1609.0	11.546, 9.279, 0.953	9.8

Table S4. *CASSCF+RASSI-SO computed relative energies of eight low lying KDs and g tensors of eight low lying KDs for Models a-c, along with deviations from the principal magnetization axes of the first KD.*

M	Model a			Model b			Model c		
	E cm^{-1}	gx, gy, gz	(°)	E cm^{-1}	gx, gy, gz	(°)	E cm^{-1}	gx, gy, gz	(°)
1	0.0	0.00, 0.00, 20.00		0.0	0.00, 0.00, 20.00		0.0	0.00, 0.00, 20.00	
2	614.1	0.00, 0.00, 16.97	0.8	590.7	0.00, 0.00, 17.00	1.7	648.4	0.00, 0.00, 16.96	2.0
3	1236.1	0.00, 0.00, 14.00	0.1	1149.7	0.00, 0.00, 14.10	2.5	1113.3	0.00, 0.00, 14.26	4.6
4	1762.0	0.04, 0.05, 11.24	1.8	1603.2	0.01, 0.01, 11.46	5.6	1424.3	0.04, 0.05, 11.64	5.1
5	2058.7	7.20, 6.54, 3.34	100.8	1884.4	0.10, 0.11, 9.58	23.9	1637.4	0.40, 0.45, 8.99	2.5
6	2120.0	9.68, 6.11, 0.13	179.2	1996.3	0.23, 0.66, 12.01	64.6	1783.7	0.88, 1.90, 6.25	1.7
7	2216.3	0.99, 3.22, 15.61	84.9	2037.7	1.32, 3.25, 8.96	75.6	1872.4	8.55, 7.28, 2.92	3.1
8	2308.4	0.32, 0.49, 19.34	97.7	2072.7	12.90, 7.20, 1.22	16.1	1947.2	0.51, 1.87, 17.89	92.0

Table S5. Important structural parameters for optimized Gd-O-Sc encapsulated all studied EMFs. Relative energies for all the four isomers of $GdOSc@C_{76}$ are also reported

Molecules	Gd-O (Å)	Sc-O (Å)	Gd-O-Sc (°)	Gd-Sc (Å)	Relative Energies (kJ/mol)
GdScO-C_{72}	2.13	1.91	179.8	4.05	
GdScO-C_{76}-1	2.14	1.91	161.3	3.99	6.3
GdScO-C_{76}-2	2.13	1.87	166.7	3.97	22.0
GdScO-C_{76}-3	2.08	1.86	131.3	3.59	0.0
GdScO-C_{76}-4	2.07	1.86	133.4	3.61	42.9
GdScO-C_{82}	2.08	1.86	151.1	3.82	

Table S6. *CASSCF+RASSI-SO computed relative energies of eight low lying KDs and g tensors of eight low lying KDs for DyOSc@C_{72}-2, DyOSc@C_{72}-3 and DyOSc@C_{72}-4 molecules, along with deviations from the principal magnetization axes of the first KD.*

M	*DyOSc*@C_{76}-2			*DyOSc*@C_{76}-3			*DyOSc*@C_{76}-4		
	E cm^{-1}	gx, gy, gz	(°)	E cm^{-1}	gx, gy, gz	(°)	E cm^{-1}	gx, gy, gz	(°)
1	0.0	0.000, 0.00, 19.958		0.0	0.000, 0.00, 19.962		0.0	0.000, 0.00, 19.962	
2	389.6	0.001, 0.001, 17.108	2.9	416.4	0.002, 0.002, 17.101	3.7	415.8	0.002, 0.002, 17.098	3.3
3	758.9	0.054, 0.060, 14.324	3.4	820.3	0.024, 0.029, 14.285	2.9	821.9	0.024, 0.028, 14.282	2.6
4	1044.0	0.312, 0.398, 11.567	2.3	1137.6	0.059, 0.085, 11.560	0.4	1141.3	0.053, 0.080, 11.558	0.2
5	1231.0	2.273, 2.404, 8.487	2.4	1340.8	0.550, 1.213, 8.822	13.1	1345.6	0.458, 1.147, 8.787	12.8
6	1319.3	3.274, 6.617, 10.977	86.3	1421.1	2.901, 7.107, 12.114	79.2	1426.0	11.880, 7.434, 2.889	9.8
7	1375.6	1.049, 2.761, 17.146	89.0	1462.8	0.160, 0.418, 17.169	94.1	1466.9	0.118, 0.278, 17.266	93.7
8	1405.5	0.504, 2.106, 16.607	91.4	1538.4	0.227, 1.480, 18.434	90.3	1539.9	0.218, 1.567, 18.346	90.2

Table S7. Magneto-structural correlation of anisotropy properties by varying Dy-O-Lu angle in Model-a from 100 to 180°.

100				
E cm^{-1}	**gx,**	**gy,**	**gz**	**(°)**
0.0	0.00	0.00	20.00	
645.0	0.00	0.00	16.95	1.9
1279.7	0.00	0.00	13.98	3.7
1808.6	0.12	0.16	11.16	6.9
2087.2	4.10	5.37	10.63	85.6
2187.9	0.32	1.41	11.28	90.0
2346.4	0.62	1.44	16.20	90.4
2524.6	0.08	0.15	19.52	80.4

120				
E cm^{-1}	**gx,**	**gy,**	**gz**	**(°)**
0.0	0.00	0.00	20.01	
611.4	0.00	0.00	16.98	1.6
1227.1	0.00	0.00	14.02	2.7
1748.9	0.02	0.02	11.29	4.6
2055.2	2.43	4.40	7.86	25.6
2124.0	8.96	8.53	0.98	3.3
2216.3	1.15	3.61	15.19	87.9
2290.9	0.29	0.55	19.34	82.2

140				
E cm^{-1}	**gx,**	**gy,**	**gz**	**(°)**
0.0	0.00	0.00	20.01	
596.8	0.00	0.00	17.00	1.4
1206	0.00	0.00	14.03	2.1
1725	0.02	0.02	11.30	3.2
2032.9	1.65	2.73	8.26	21.1
2094	11.27	7.42	1.17	3.1
2171.1	1.06	4.95	14.38	89.0
2218.3	0.70	1.21	19.13	85.8

160				
E cm^{-1}	**gx,**	**gy,**	**gz**	**(°)**
0.0	0.00	0.00	20.01	
593.1	0.00	0.00	17.00	1.0
1202.5	0.00	0.00	14.03	1.3
1722.6	0.02	0.02	11.30	1.6
2029.5	1.81	3.11	8.06	18.2
2082.7	11.39	7.35	0.89	2.3

2157.0	0.91	5.70	13.84	88.1
2199.0	1.02	1.59	18.87	90.0

180				
E cm^{-1}	**gx,**	**gy,**	**gz**	**(°)**
0.0	0.00	0.00	20.01	
588.7	0.00	0.00	17.0	1.0
1196.2	0.00	0.00	14.03	1.0
1715.6	0.00	0.00	11.30	0.6
2021.2	2.19	4.05	7.57	179.1
2074.0	10.61	7.82	0.68	1.6
2149.9	1.04	5.31	14.23	85.0
2199.3	0.81	1.27	19.00	86.1

Computational Details:

In case of $Gd_2O@C_{xy}$ (xy = 72, 76 and 82) cage, the magnetic exchange interaction between Gd^{3+} ions are described by the following spin Hamiltonian,

$$\hat{H} = -JS_{Gd1}S_{Gd2}$$

Here *J* is the isotropic exchange coupling constant and S_{Gd1} and S_{Gd2} are spins on Gd^{III} (S=7/2) and fullerene radical (S=1/2) atoms respectively. The DFT calculations combined with Broken Symmetry (BS) approach[1] has been employed to compute the *J* values. Here, we have performed most of our calculations using Gaussian 09 suite of programs.[2] All of the molecules were geometry optimized at the UB3LYP functional[3] with a 6-31G* basis set[4a] for carbon and oxygen atoms, Lanl2DZ basis set,[5b] which encompasses a double-ζ quality basis set with the Los Alamos effective core potential, for Sc atom and with a double-zeta quality basis set employing Cundari-Stevens (CS) relativistic effective core potential for gadolinium atoms.[5] For single point calculations, we have employed spin-unrestricted B3LYP functional along with a double-zeta quality basis set employing Cundari-Stevens (CS) relativistic effective core potential on Gd atom[5] and TZV basis set[6] for the rest of the atoms (Sc, C, O) for single point calculation. A very tight SCF convergence has been employed throughout to attain SCF convergence upto $1x10^{-8}$ h.

For the incorporation of anisotropy in the molecule, we have replaced one Gd(III) ions with anisotropic Dy(III) ions other one by isotropic Lu(III) ion. In second case, we have DyOSc cluster encapsulated inside fullerenes.

All the *ab initio* calculations have been performed using MOLCAS 8.0 code. Here we have employed the ANO...RCC VTZP basis set for Dy atoms, the ANO...RCC VTZ basis set for Sc and O, and the ANO...RCC VDZP basis set for Lu and C atoms. The ground state f-electron configuration for Dy(III) is $4f^9$ with $^6H_{15/2}$ multiplet as a ground state. First, we have generated the guess orbitals from there we have selected seven Dy(III) based starting orbitals to perform the CASSCF calculations. CASSCF calculations have been performed where eleven electrons are in the seven active orbitals with an active space of CAS(9,7). Using this active space first we have computed 21 sextets using the configuration interaction (CI) procedure. After this, we have performed RASSI-SO module to compute the spin-orbit coupled states. After computing these SO states, we have performed the SINGLE_ANISO code to extract the corresponding g-tensors. Here we have computed the g-tensors for the eight low-lying Kramers Doublets. The cholesky decomposition for two electron integrals is employed throughout in the calculations to reduce the disk space.

References.

1. a) L. Noodleman, *J. Chem. Phys.*, 1981, **74**, 5737; b) L. Noodleman and E. R. Davidson, *Chem. Phys.*, 1986, **109**, 131; c) L. Noodleman and D. A. Case, *Adv. Inorg.Chem.*, 1992, **38**, 423; d) L. Noodleman and J. G. Norman, *J. Chem. Phys.*, 1979, **70**, 4903.
2. M. J. Frisch, G. W. Trucks, H. B. Schlegel, G. E. Scuseria, M. A. Robb, J. R. Cheeseman, G. Scalmani, V. Barone, B. Mennucci, G. A. Petersson, H. Nakatsuji, M. Caricato, X. Li, H. P. Hratchian, A. F. Izmaylov, J. Bloino, G. Zheng, J. L. Sonnenberg, M. Hada, M. Ehara, K. Toyota, R. Fukuda, J. Hasegawa, M. Ishida, T. Nakajima, Y. Honda, O. Kitao, H. Nakai, T. Vreven, J. A. Montgomery, J. E. Peralta, F. Ogliaro, M. Bearpark, J. J. Heyd, E. Brothers, K. N. Kudin, V. N. Staroverov, R. Kobayashi, J. Normand, K. Raghavachari, A. Rendell, J. C. Burant, S. S. Iyengar, J. Tomasi, M. Cossi, N. Rega, J. M. Millam, M. Klene, J. E. Knox, J. B. Cross, V. Bakken, C. Adamo, J. Jaramillo, R. Gomperts, R. E. Stratmann, O. Yazyev, A. Austin, J. R. Cammi, C. Pomelli, J. W. Ochterski, R. L. Martin, K. Morokuma, V. G. Zakrzewski, G. A. Voth, P. Salvador, J. J. Dannenberg, S. Dapprich, A. D. Daniels, Ö. Farkas, J. B. Foresman, J. V. Ortiz, J. Cioslowski and D. J. Fox, *Gaussian 09*, 2009.
3. a) C. Lee, W. Yang and R. G. Parr, *Phys. Rev. B: Condens. Matter*, 1988, **37**, 785; b) A. D. Becke, *J. Chem. Phys.*, 1993, **98**, 5648; c) A. D. Becke, *J. Chem. Phys.*, 1993, **98**, 1372; d) P. J. Stephens, F. J. Devlin, C. F. Chabalowski and M. J. Frisch, *J. Phys. Chem.*, 1994, **98**, 11623-11627.
4. P. C. Hariharan and J. A. Pople, *Theoret. Chim. Acta*, 1973, **28**, 213-222.
5. T. R. Cundari and W. J. Stevens, *J. Chem. Phys.*, 1993, **98**, 5555-5565.
6. a) A. Schaefer, H. Horn and R. Ahlrichs, *J. Chem. Phys.*, 1992, **97**, 2571; b) A. Schaefer, C. Huber and R. Ahlrichs, *J. Chem. Phys.*, 1994, **100**, 5829; c) G. E. Scuseria and H. F. Schaefer, *III J. Chem. Phys.*, 1989, **90**, 3700.
7. F. Aquilante, L. De Vico, N. Ferré, G. Ghigo, P.-å. Malmqvist, P. Neogrády, T. B. Pedersen, M. Pitoňák, M. Reiher, B. O. Roos, L. Serrano-Andrés, M. Urban, V. Veryazov and R. Lindh, *J. Comput. Chem.*, 2010, **31**, 224-247.